Three-dimensional solitons in two-component Bose–Einstein condensates*

Liu Yong-Kai(刘永恺)[a] and Yang Shi-Jie(杨师杰)[a)b)†]

[a] Department of Physics, Beijing Normal University, Beijing 100875, China

[b] State Key Laboratory of Theoretical Physics, Institute of Theoretical Physics, Chinese Academy of Sciences, Beijing 100190, China

(Received 25 April 2014; revised manuscript received 27 June 2014; published online 17 September 2014)

We investigate a kind of solitons in the two-component Bose–Einstein condensates with axisymmetric configurations in the $R^2 \times S^1$ space. The corresponding topological structure is referred to as Hopfion. The spin texture differs from the conventional three-dimensional (3D) skyrmion and knot, which is characterized by two homotopy invariants. The stability of the Hopfion is verified numerically by evolving the Gross–Pitaevskii equations in imaginary time.

Keywords: two-component Bose–Einstein condensates, three-dimensional (3D) soliton, coupled Gross–Pitaevskii equations, Hopfion

PACS: 03.75.Mn, 03.75.Lm, 67.85.Fg **DOI:** 10.1088/1674-1056/23/11/110308

1. Introduction

The knot structure has been a fascinating subject for decades and it has been discussed in various fields of physics, ranging from condensed matter physics[1–4] to optics[5–7] and the classical field theory.[8,9] Knots have linking numbers, which are classified by the third homotopy $\pi_3(S^2)$.[10] Other familiar topological excitations, such as vortices and skyrmions, are classified by the winding numbers.[11,12] The knot invariants can be calculated by determining the linking number of the preimage of two distinct points, which can see intuitively from the image. In addition, Hopfions have been widely investigated in the Faddeev–Skyrme (FS) model.[13–15] In comparison, the relevant properties in condensed matter physics, especially the Bose–Einstein condensates (BECs), are rarely addressed.[2] One of the obstacles is the stability or lifetime of a knot in the BECs. In a recent paper,[16] the winding Hopfions on $R^2 \times S^1$ were found to be stable in the FS model for the linear potential $V_1 = m^2(1-n_3)$ or the antiferromagnetic potential $V_2 = m^2(1-n_3^2)+\beta^2 n_1$.

Motivated by this finding, we have attempted to examine whether this kind of topological structure can be stabilized in the BECs. As we know, the BECs provide an ideal testing ground for exotic topological solitons in a quantum condensed system.[11,17–19] The optical techniques can be used to control and directly visualize the condensate wave functions.[20] Two-dimensional (2D) skyrmions and knots with finite lifetime in the BECs have been created and observed experimentally.[2,21] For a conventional three-dimensional (3D) two-component BEC, the spin field $\boldsymbol{S}(\boldsymbol{x})$ defines a map from a 3D domain $(\boldsymbol{x})$ into a 2D sphere. Consequently, the preimage of a point on the target S^2 corresponds to a closed loop in S^3, provided that the manifold space is compact. If the $\boldsymbol{S}$ field has a Hopf charge $Q_{\rm H}$, then two loops corresponding to the preimages of any two distinct points on the target S^2 will be linked $Q_{\rm H}$ times.[10] Such mappings fall into nontrivial homotopy classes $\pi_3(S^2) \cong Z$ and can be characterized by a topological invariant that is called the Hopf invariant. The Hopf invariant is $Q_{\rm H} = \frac{1}{4\pi^2}\int \varepsilon_{ijk}\mathcal{F}_{ij}\mathcal{A}_k \,{\rm d}^3x$, where $\mathcal{F}_{ij} = \partial_i\mathcal{A}_j - \partial_j\mathcal{A}_i = \boldsymbol{S}\cdot(\partial_i\boldsymbol{S}\times\partial_j\boldsymbol{S})$.[2]

In this paper, we study the Hopfions formed by a twisted baby skyrmion and verify their stabilities in a two-component BEC on $R^2 \times S^1$, where S^1 represents the periodic condition in the z direction. However, in this case the Hopf number is not a homotopy invariant, although such a configuration carries a Hopf number as in R^3.[14,16] Virtually, the map is classified by two homotopy invariants from the point of view of topology.

The rest of this paper is organized as follows. In Section 2, we describe the model of the two-component BEC. In Section 3, we explore the topology of $S^2 \times S^1 \to S^2$. In Section 4, we numerically examine the stability of the Hopfion. A brief summary is included in Section 5.

2. Model

The system considered here is a two-component BEC confined in a 2D trap and which is periodic in the z direction. The dynamics of the system is described by the coupled Gross–Pitaevskii equations (GPEs)

$$\mathrm{i}\hbar\frac{\partial\psi_i}{\partial t} = \left(-\frac{\hbar^2}{2m}\nabla^2 + V(\boldsymbol{r}) + \sum_{j=1,2}U_{ij}|\psi_j|^2\right)\psi_i, \qquad (1)$$

where ψ_i $(i=1,2)$ denote the wave functions of the two components, which are normalized to the number of atoms in each

*Project supported by the National Natural Science Foundation of China (Grant No. 11374036) and the National Basic Research Program of China (Grant No. 2012CB821403).

†Corresponding author. E-mail: yangshijie@tsinghua.org.cn

© 2014 Chinese Physical Society and IOP Publishing Ltd

component, N_1 and N_2. The external trap is taken as an axisymmetric harmonic potential $V(\boldsymbol{r}) = \frac{1}{2}m\omega^2(x^2+y^2)$. The coupling constants $U_{ij} = 4\pi\hbar^2 a_{ij}/m$ represent the atom–atom interactions.[22]

In order to simplify the equations, we adopt the dimensionless coupled GPEs.[22] By substituting $\psi_i(x,y,z,t) = \psi_i(x,y,z)\exp(-\mathrm{i}\mu_i t)$, the stationary equations read

$$\mu_1\psi_1 = \left(-\frac{1}{2}\nabla^2 + V(\boldsymbol{r}) + \gamma_{11}|\psi_1|^2 + \gamma_{12}|\psi_2|^2\right)\psi_1,$$
$$\mu_2\psi_2 = \left(-\frac{1}{2}\nabla^2 + V(\boldsymbol{r}) + \gamma_{22}|\psi_2|^2 + \gamma_{21}|\psi_1|^2\right)\psi_2. \quad (2)$$

We construct an ansatz wavefunction which is the exact solution to the GPEs in the limit of vanishing nonlinear interactions ($\gamma_{ij} = 0$). It is expressed in the cylindrical coordinates as

$$\psi = \mathrm{e}^{-\frac{1}{2}\rho^2}\begin{pmatrix}\mathrm{e}^{\mathrm{i}k_n z}\\ \rho^m \mathrm{e}^{\mathrm{i}m\theta}\end{pmatrix}. \quad (3)$$

The order parameter (OP) of the two-component BEC is represented by a normalized spinor $\boldsymbol{\xi}(\boldsymbol{r})$ as $\psi(\boldsymbol{r}) = \sqrt{n(\boldsymbol{r})}\boldsymbol{\xi}(\boldsymbol{r})$, where $n(\boldsymbol{r})$ is the condensate density.[10,23] It can be parameterized as[24]

$$\begin{pmatrix}\psi_1\\ \psi_2\end{pmatrix} = \sqrt{n(\boldsymbol{r})}\begin{pmatrix}\cos(\beta(\boldsymbol{r}))\,\mathrm{e}^{\mathrm{i}\phi_1(\boldsymbol{r})}\\ \sin(\beta(\boldsymbol{r}))\,\mathrm{e}^{\mathrm{i}\phi_2(\boldsymbol{r})}\end{pmatrix}, \quad (4)$$

where $\beta \in [0,\pi/2]$ and $\phi_1, \phi_2 \in [0,2\pi]$. Through studying the OP, we can investigate the types of topological excitations. The pseudospin is constructed by $\boldsymbol{S} = \boldsymbol{\xi}^\dagger\boldsymbol{\sigma}\boldsymbol{\xi}$, where $\boldsymbol{\sigma}$ is the Pauli matrix.

3. Topology

In contrast to the previous works on BECs,[2] in which the authors considered the knots in R^3 and defined the Hopf mapping $\pi_3(S^2)$, we consider a similar configuration but enforce the periodicity condition in the z direction. Since the one-point compactification of R^2 is S^2, the physical space is then $S^2 \times S^1$. The homotopy classification of the above case is more complicated than the usual case of $S^3 \to S^2$. Globally, S^3 is distinct from $S^2 \times S^1$. The first homology group of the space is $H_1(S^2 \times S^1) = Z$, while $H_1(S^3) = 0$.[25] As to the map $S^2 \times S^1 \to S^2$, we have a primary invariant q related to $S^2 \to S^2$ and a secondary invariant Z_{2q}.[14,16]

In order to obtain a better understanding of the situation, we can consider a physical picture of a twisted baby skyrmion string: a baby skyrmion with 2D skyrmion number q winding around S^1, along which the phase modulus is twisted p times. While such a configuration carries the Hopf number pq, neither the twisting p nor the Hopf number pq is a homotopy invariant. Instead, we find that q and p modulo $2q$ are homotopy invariants. The new invariants are given by the induced map on the second cohomology. The relative number of twists is only a well defined modulo $2q$ for q depending on the cohomology class $\varphi^*\mu_{S^2} \in H^2(M;Z)$, where μ_{S^2} is a generator of $H^2(S^2;Z)$. We can have an intuitive view in Fig. 5.[26] If $q \neq 0$, there are $2q$ different homotopy classes corresponding to the same degree. For example, there are two homotopy classes for $q = 1$: a configuration with $(p,q) = (2,1)$ can be continuously deformed into a configuration with $(p,q) = (0,1)$, even the linking number is zero for the former and two for the latter. Although it seems impossible to deform $(2,1) \to (0,1)$ by continuous deformation from the first impression, the higher numbers of twists can indeed be unwound from the point view of topology.[14]

4. Stability

In addition to the topology, we should examine the stability of the energy. Using the trial function (3), we obtain a stable 3D soliton with nearly the same shape of the initial wavefunction during the imaginary time evolution[27–30] as shown in Fig. 1 for $m = 1$. Figure 1 shows the density and the phase profile of the 3D numerical soliton for $\gamma_{11} = \gamma_{22} = \gamma_{12} = \gamma_{21}$, where the system possesses the SU(2) symmetry. However, we can also obtain the same stable solution with a finite difference between the intracomponent and the intercomponent interactions.

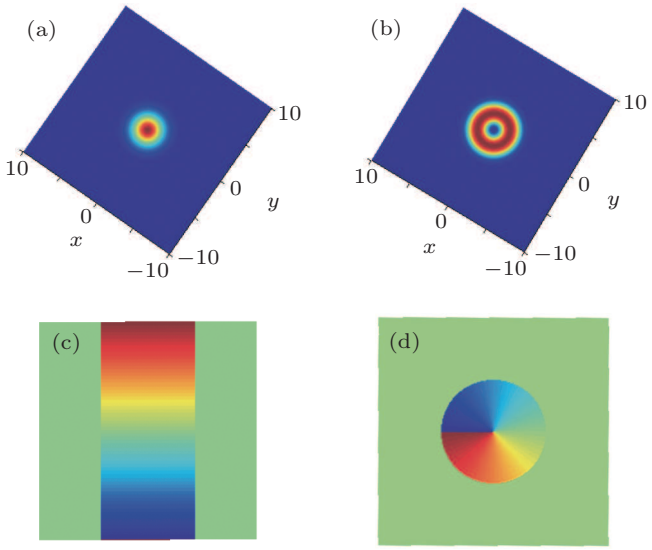


Fig. 1. (color online) The density profiles of (a) ψ_1 and (b) ψ_2 in the x–y plane. (c) The phase distribution of ψ_1 in the x–z plane and (d) that of ψ_2 in the x–y plane. The parameters are $\gamma_{11} = \gamma_{22} = \gamma_{12} = \gamma_{21} = 1000$.

By introducing the OP, we can give conduct a detailed analysis of a stable soliton to study the structure. Here, we choose the ansatz $\beta = q_r f(r)$, $\phi_1 = p2\pi z/L_z = pg(z)$, $\phi_2 = q_\theta\theta$, with the integers p, q_r, q_θ and the cylindrical coordinates (r,θ,z).[16] The function $f(r)$ satisfies the boundary condition $f(r \to 0) = 0$, $f(r \to \infty) = \pi/2$, and the function $g(z)$ satisfies

the boundary condition $g(z\to 0)=0$, $g(z\to L_z)=2\pi$. The explicit expressions of the pseudospin $\boldsymbol{S}=(S_x,S_y,S_z)$ are given by

$$\begin{aligned} S_x &= \xi_1^*\xi_2+\xi_2^*\xi_1=\sin(2q_rf(r))\cos(pg(z)-q_\theta\theta),\\ S_y &= -\mathrm{i}(\xi_1^*\xi_2-\xi_2^*\xi_1)=-\sin(2q_rf(r))\sin(pg(z)-q_\theta\theta),\\ S_z &= (\xi_1^*\xi_1-\xi_2^*\xi_2)=\cos(q_rf(r))^2-\sin(q_rf(r))^2. \end{aligned} \tag{5}$$

Let us first examine the 2D situation at each slice of constant z. This is constructed by mapping the two-dimensional space with a uniform boundary to the S^2 target space for $\boldsymbol{S}$, which exhibits a 2D skyrmion (baby skyrmion), as shown in Fig. 2. It is known that the 2D skyrmion has a topological invariant defined in the two-dimensional system as

$$\begin{aligned} Q_{2\mathrm{D}} &= \frac{1}{4\pi}\int \boldsymbol{S}\cdot(\partial_x\boldsymbol{S}\times\partial_y\boldsymbol{S})\,\mathrm{d}\boldsymbol{r}\\ &= \frac{q_\theta}{4\pi}\int_0^\infty \mathrm{d}r\int_0^{2\pi}\mathrm{d}\theta\sin(2q_rf(r))2q_rf'(r)\\ &= \frac{q_\theta[1-(-1)^{q_r}]}{2}. \end{aligned}$$

From this, we can see that, $Q_{2\mathrm{D}}=0$ for the even values of q_r, and $Q_{2\mathrm{D}}=q_\theta$ for the odd values. During the numerical calculations, we take $q_r=1$ and $q=q_\theta$. Figure 2 shows the 2D skyrmion with $q=1$ in the ρ–φ plane. We find no stable states for $q_r>1$.

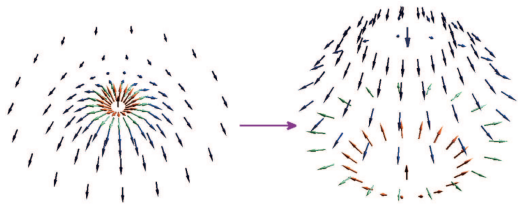


Fig. 2. (color online) The spin texture in R^2 whose boundary is identified in the sphere S^2.

To obtain the 3D numerical solitons, we start from the initial solution Eq. (3) with $q_r=1$. During our calculation, we give numerical solutions for the ψ_1 phase modulus that is twisted not less than three times along the z direction, under the situation that the ψ_2 component has one singly quantized vortex and multiply quantized vortexes. Namely, we give numerical solutions for $q=1,2,3$ and $p=1,2,3$.

Next ,we further explore the 3D structure constructed from the 2D skyrmions. As the 2D skyrmion can be parameterized as S^2 in our case, the 3D structure forms a twisted string, which is periodic in the z direction and can be represented by concentric spheres. The map $S^2\times[0,2\pi]\to S^2$ is displayed in Fig. 3, where 0 and 2π denote the boundary condition. The preimages make a braid structure with the numerical solutions shown in Fig. 3(a) for $(p,q)=(1,1)$ and in Fig. 3(b) for $(p,q)=(1,2)$. Here, the tube describes the preimages of $S_i=0.98$, where we plot a small isosurface around one point $\boldsymbol{S}$. In Fig. 3(a), the twisted tubes describe two distinct preimages of the points on the target S^2 having linking number 1. The linking number is 2 in Fig. 3(b). Although we have a linking number, it is not a homotopy invariant in this case, as discussed in Section 3.

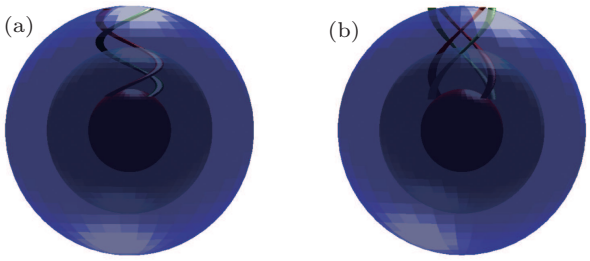


Fig. 3. (color online) These pictures illustrate the map $S^2\times[0,2\pi]\to S^2$ between the innermost (red), the middle (cyan), and the outermost (blue) spheres. The twist tubes (red and green) represent small isosurfaces around two distinct points for (a) $(p,q)=(1,1)$ and (b) $(p,q)=(1,2)$.

For our case, even though the Hopf number is not the homotopy invariant on $R^2\times S^1$, we still have the same mathematical definition such as in R^3 by integrating over $R^2\times S^1$ (we may consider an injection $R^2\times S^1\to S^3$). The Hopf number for $\boldsymbol{S}$ parametered S^2 is

$$Q_{\mathrm{H}}=\frac{1}{4\pi^2}\int_{R^2\times S^1}\varepsilon_{ijk}\mathcal{F}_{ij}\mathcal{A}_k\,\mathrm{d}^3x=pq, \tag{6}$$

where $\mathcal{F}_{ij}=\partial_i\mathcal{A}_j-\partial_j\mathcal{A}_i=\boldsymbol{S}\cdot(\partial_i\boldsymbol{S}\times\partial_j\boldsymbol{S})$. We can obtain that the Hopf number or linking number is the product of 2D skyrmion number q and U(1) modulus twisting p, which is related to the homotopy invariants discussed in Section 3.

Next, we look at the twist tubes. From knot and braid theory we can find that every torus knot has a representation in terms of a braid program. In contrast, in order to obtain a more intuitive view of the linking number, we plot the spin texture in the image of a torus with the ends identified.[31] For example, the twist tubes in Fig. 3(a) correspond to the torus in Fig. 4(a). Figure 4 displays the isosurfaces of $S_x=0.98$ and $S_y=0.98$ of the numerical solutions with different (p,q) in the image of torus. One can easily count the linking number to be pq for $q=1$ (Figs. 4(a), 4(d), and 4(g)). For a larger q, the crossings are too many and complicated to count directly. In this case, the linking number can also be determined by the twist plus writhe in the torus knot. For example, figure 5 shows an alternative description for Fig. 4(h). Figure 5(a) shows a torus and a tube corresponding to the image of $S_z=0$ and one nearby point of the numerical solution with $(p,q)=(3,2)$. From the ribbon view suggested by Hietarinta, the twist and the writhe are both 3 in Fig. 5(a), so the linking number is 6. This tube is different from the unknot that was discussed previously. In Fig. 5(b), we show that the tube in Fig. 5(a) is exactly a trefoil knot, which is the simplest example of a nontrivial knot.

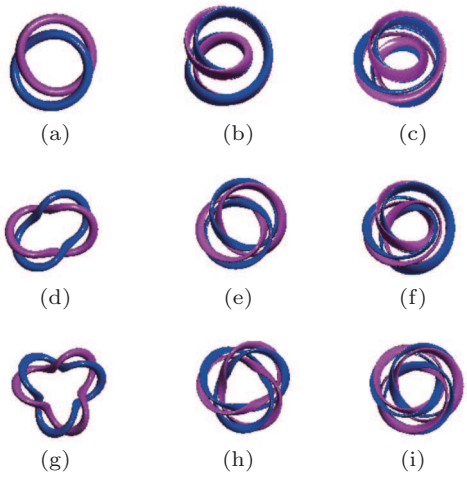


Fig. 4. (color online) The torus images of $S_x = 0.98$ (red) and $S_y = 0.98$ (blue) of our numerical solutions of different (p,q): (a) (1, 1), (b) (1, 2), (c) (1, 3), (d) (2,1), (e) (2, 2), (f) (2, 3), (g) (3, 1), (h) (3, 2), and (i) (3, 3).

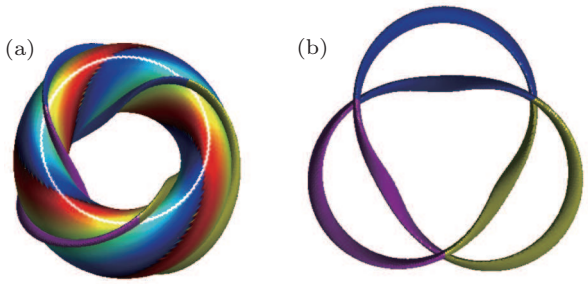


Fig. 5. (color online) (a) The torus corresponds to the image of $S_z = 0$, and the small tube is the image of one nearby point for $(p,q) = (3,2)$. (b) The small tube is just the trefoil knot.

5. Summary

We have numerically investigated the 3D solitons in a two-component BEC on $R^2 \times S^1$. From the point view of topology, the mapping $S^2 \times S^1 \to S^2$ has two homotopy invariants. However this is only a mathematic definition. For a specific physical system, our solution with $(p,q) = (2,1)$ is at least at local minimum, implying an energy barrier to $(p,q) = (0,1)$. During our numerical calculations, the quantum numbers p, q and Hopf number pq do not change. These kinds of 3D solitons are energetically stable in the trapped BEC. However, constructing the 3D solitons might not be a simple task at the present moment. Recently, we have noticed a spin rotation method which has been successful used in creating 2D skyrmions, and the experimental technique can be extended to create other exotic spin textures, such as knots and monopoles in 3D condensates.[21]

References

[1] Babaev E, Faddeev L D and Niemi A J 2002 *Phys. Rev. B* **65** 100512
[2] Kawaguchi Y, Nitta M and Ueda M 2008 *Phys. Rev. Lett.* **100** 180403
[3] Zhou X, Li Y, Cai Z and Wu C 2013 *J. Phys. B: At. Mol. Opt. Phys.* **46** 134001
[4] Li Y, Zhou X and Wu C 2012 *arXiv:* 1205.2162
[5] Irvine W T M and Bouwmeester D 2008 *Nat. Phys.* **4** 716
[6] Dennis M R, King R P, Jack B, O'Holleran K and Padgett M J 2010 *Nat. Phys.* **6** 118
[7] Desyatnikov A S, Buccoliero D, Dennis M R and Kivshar Y S 2012 *Sci. Rep.* **2** 771
[8] Faddeev L and Niemi A J 1997 *Nature* **387** 58
[9] Battye R A and Sutcliffe P M 1998 *Phys. Rev. Lett.* **81** 4798
[10] Kawaguchi Y and Ueda M 2012 *Phys. Rep.* **520** 253
[11] Kawaguchi Y, Kobayashi M, Nitta M and Ueda M 2010 *Prog. Theor. Phys. Suppl.* **186** 455
[12] Zhang C, Guo W A, Feng S P and Yang S J 2013 *Chin. Phys. B* **22** 110308
[13] Gladikowski J and Hellmund M 1997 *Phys. Rev. D* **56** 5194
[14] Jäykkä J and Hietarinta J 2009 *Phys. Rev. D* **79** 125027
[15] Kobayashi M and Nitta M 2014 *Phys. Lett. B* **728** 314
[16] Kobayashi M and Nitta M 2013 *Nucl. Phys. B* **876** 605
[17] Liu X X, Zhang X F and Zhang P 2010 *Chin. Phys. Lett.* **27** 070306
[18] Ian M S, Wu C J and Zhou X F 2011 *Chin. Phys. Lett.* **28** 097102
[19] Cui G D, Sun J F, Jiang B N, Qian J and Wang Y Z 2013 *Chin. Phys. B* **22** 100501
[20] Kasamatsu K, Takeuchi H, Tsubota M and Nitta M 2013 *Phys. Rev. A* **88** 013620
[21] Choi J Y, Kwon W J and Shin Y I 2012 *Phys. Rev. Lett.* **108** 035301
[22] Wüster S, Argue T E and Savage C M 2005 *Phys. Rev. A* **72** 043616
[23] Mäkelä H 2006 *J. Phys. A: Math. Gen.* **39** 7423
[24] Battye B A, Cooper N R and Sutcliffe P M 2002 *Phys. Rev. Lett.* **88** 080401
[25] Ryder L H 1980 *J. Phys. A: Math. Gen.* **13** 437
[26] Auckly D and Speight M 2006 *Commun. Math. Phys.* **263** 173
[27] Bao W, Jaksch D and Markowich P A 2003 *J. Comput. Phys.* **187** 318
[28] Bao W and Wang H 2006 *J. Comput. Phys.* **217** 612
[29] Yang S J, Wu Q S, Zhang S N and Feng S 2008 *Phys. Rev. A* **77** 033621
[30] Bao W and Cai Y 2013 *Kinet. Relat. Mod.* **6** 1
[31] Liu Y K and Yang S J 2013 *Phys. Rev. A* **87** 063632